



## A multinuclear static NMR study of geopolymerisation



Aurélie Favier <sup>a,\*</sup>, Guillaume Habert <sup>b</sup>, Nicolas Roussel <sup>a</sup>, Jean-Baptiste d'Espinoze de Lacaille <sup>c</sup>

<sup>a</sup> Univ Paris-Est, IFSTTAR, Materials Department, 14-20 bd Newton, F-77447 Marne la Vallée Cedex 2, France

<sup>b</sup> Institute for Construction and Infrastructure Management, ETH Zurich, CH-8093 Zurich, Switzerland

<sup>c</sup> Ecole Supérieure de Physique et de Chimie Industrielles de la Ville de Paris (ESPCI), ParisTech, PSL Research University, Soft Matter Sciences and Engineering Laboratory SIMM, CNRS UMR 7615, 10 rue Vauquelin, F-75005 Paris, France

### ARTICLE INFO

#### Article history:

Received 4 November 2014

Accepted 3 March 2015

Available online 29 May 2015

#### Keywords:

Rheology

Spectroscopy

Alkali activated cement

Metakaolin

Reaction

### ABSTRACT

Geopolymers are inorganic binders obtained by alkali activation of aluminosilicates. While the structure of geopolymers is now well understood, the details of the geopolymerisation reaction and their impact on the rheology of the paste remain uncertain. In this work, we follow the elastic properties of a paste made with metakaolin and sodium silicate solution. After the first sharp increase of elastic modulus occurring a few hundred of seconds after mixing and related to the heterogeneous formation of an alumina–silicate gel with a molar ratio Si/Al < 4 located at the grains boundaries, we focus on the progressive increase in elastic modulus on a period of few hours during the setting of the geopolymer. In this study, we combine the study of rheological properties of the paste with <sup>23</sup>Na, <sup>27</sup>Al and <sup>29</sup>Si static NMR measurement in order to better understand the origin of this second increase in elastic modulus. Our results show that, after a few hours, Al and Na evolution in the liquid phase are concomitant. This suggests the precipitation of an aluminosilicate phase where Al is in tetrahedral position and Na compensates the charge. Furthermore, Si speciation confirms this result and allows us to identify the precipitation of a product, which has a chemical composition close to the final composition of geopolymer. This study provides strong evidence for a heterogeneous formation of an aluminosilicate glass directly from the first gel and the silicate solution without the need for a reorganisation of Gel 1 into Gel 2.

© 2015 Elsevier Ltd. All rights reserved.

### 1. Introduction

It is expected that the demand for concrete continues to grow especially in developing countries [1]. These forecasts shall result in increased emissions of greenhouse gases generated during the manufacture of Portland cement. To reduce the environmental footprint of construction industries, the development of sustainable building materials is essential. Several solutions have emerged in recent years such as the blended cements, in which parts of clinker is substituted by Supplementary Cementitious Materials (SCMs) [2,3]. Other Non-Portland based cements such as calcium aluminate cements [4–6], magnesia cements [7,8] or alkali activated binders including geopolymers attract a lot of scientific attention. Indeed, for the last decades, aluminosilicate materials, also known as geopolymers [9], have been largely studied due to their promising potential applications as environmentally friendly alternatives to Portland cement [10–13]. The interest they could provide for waste remediation and in particular nuclear waste or heavy metals containment have also motivated intensive research on this field since the last 20 years [14,15]. These amorphous aluminosilicate

materials are typically synthesised under highly alkaline conditions from a solid aluminosilicate such as fly ash, slag or some calcined clay such as metakaolin (MK). The resulting geopolymers consist of an X-ray amorphous three-dimensional structure with a tetrahedral coordination of AlO<sub>4</sub> and SiO<sub>4</sub> units [16,17].

Extensive research has helped to consolidate knowledge on geopolymerisation. Currently, geopolymerisation is described in literature by three main concurrent and partially reversible steps:

- (1) A dissolution step, in which the aluminosilicate source is dissolved in order to form reactive precursors such as Si(OH)<sub>4</sub><sup>-</sup> and Al(OH)<sub>4</sub><sup>-</sup>. This step is crucial for the future geopolymerisation reaction and previous works have shown that this is the limiting step of the overall reaction. There may appear differences in dissolution rate according to the Al coordination [18].
- (2) A reorganisation step, where aluminosilicate precursors rearrange towards a more stable state. This step is either described as an instantaneous step or as a long process with various types of temporary gels formed [11].
- (3) A polycondensation/gelification phase during which polymerisation and precipitation of the system occur. It involves the condensation between mono aluminate and mono silicate to

\* Corresponding author. Tel.: +41 21 693 78 52.  
E-mail address: [aurelie.favier@epfl.ch](mailto:aurelie.favier@epfl.ch) (A. Favier).

form Si—O—Si and Si—O—Al bonds since the formation of Al—O—Al is not favoured (Loewenstein's Rule) even if it is not strictly impossible [19,20].

Even if these steps are clearly described in the literature and are used in geopolymerisation models, a lot of uncertainties still remain, especially in the succession of these phases and their repetition. Does the last step involve the formation of only one final product or is there a phase of polycondensation (step 3) followed by a new phase of reorganisation (step 2) inducing again a new polymerisation phase of new products. The detailed understanding of these steps, their succession and their potential repetition is crucial for a proper understanding of the reaction. In the literature, two fundamentally different models depending on the number of reorganisation stages have been proposed. Some models describe the geopolymerisation as a linear process implying one aluminosilicate gel that polymerises from a solution of aluminate and silicate oligomers [9]. Other models favour a reorganisation of a first gel into a second gel [11,21]. To distinguish between those two options, studies have used a variety of techniques. In particular,  $^1\text{H}$  NMR relaxometry [22] provides information about the evolution of pore structure and multinuclear MAS NMR [21,23–27] gave access to the structure of short-range order encountered in geopolymers. Also, in-situ neutron pair distribution function (PDF) analysis [28–30] provided information on the local gel structure. These methods emphasized the importance of the local structure formed in the interstitial phase and the strong heterogeneity of the geopolymer gel. However, all these experiments only allowed for the assessment of the solid phases of material and not of the liquid phase.

Few studies have effectively tried to observe the interstitial phases. Studies such as [31] have mixed directly solutions of silicate and aluminate. They measured the properties of the precipitate as well as the remnant liquid. This method is however only useful if one considers a first instantaneous dissolution of the aluminate source to have in the solution mono aluminate and mono silicate species. In the reality, the continuous dissolution process of MK might induce a different reaction mechanism [18]. A second study, used static  $^{27}\text{Al}$  solution NMR to measure only the aluminium present in the solution and probe the molecular changes occurring during the synthesis [32]. This approach emphasizes the importance of aluminium chemistry during the different steps of geopolymerisation's reaction.

Inspired by the methodology proposed by Rahier et al. [32], the objective of the present study is to monitor the chemical evolution of the interstitial phase during the formation of geopolymers from metakaolin (MK) using static  $^{27}\text{Al}$ ,  $^{29}\text{Si}$  and  $^{23}\text{Na}$  NMR measurements. In parallel, the resulting macroscopic mechanical evolution of the system is assessed using oscillation rheology.

**Table 1**  
Chemical composition of geopolymer pastes expressed in molar ratios.

Sample	$\text{SiO}_2/\text{Na}_2\text{O}$ in silicate solution	$\text{H}_2\text{O}/\text{Na}_2\text{O}$	$\text{Na}_2\text{O}/\text{Al}_2\text{O}_3$	Si/Al in the final product
$\text{SiO}_2/\text{Na}_2\text{O} = 1.06$	1.06	20	0.67	1.71
$\text{SiO}_2/\text{Na}_2\text{O} = 1.6$	1.6	20	0.63	1.86

## 2. Experimental procedure

### 2.1. Raw materials and processing

Geopolymer pastes were prepared by mixing a sodium silicate solution with MK particles. The chosen MK for this research is Argical M-1000 from AGS Minéraux (France). Its BET specific surface area is equal to  $17 \text{ m}^2/\text{g}$  and the mass average diameter is approximately  $10 \mu\text{m}$ . The alkaline solutions were prepared from silica gel 60, 0.063–0.2 mm (Merck KGaA, Germany), sodium hydroxide pellets (Merck KGaA, Germany) and distilled water. They were obtained by mixing the appropriate amount of NaOH, silica gel and distilled water in a plastic bottle, which was subsequently closed to avoid evaporation and carbonation. The solutions were then allowed to cool for 24 h. The  $^{29}\text{Si}$  NMR characterisation of the sodium silicate solution showed distinct and diverse coordination state of Silicon atoms (Fig. 1). Highly depolymerised species (isolated silicon tetrahedron,  $\text{Q}^0$ ) could be identified as well as polymerised silicon oligomers (silicon tetrahedral linked by sharing one or two oxygens,  $\text{Q}^1/\text{Q}^2$ ).

Finally, as numerous studies have shown that an optimal composition of the final geopolymeric phase for structural applications and the development of mechanical properties correspond to molar ratios Si/Al close to 2 and  $\text{Na}_2\text{O}/\text{Al}_2\text{O}_3$  close to 1 [27,33], geopolymer pastes were prepared in order to be close to these values. Notwithstanding its impact on the final mechanical properties, the water content was chosen to keep the initial solid volume fraction constant and equal to 0.3 in order to allow rheological measurements comparable between each other. As a result, the alkaline solutions had a constant  $\text{H}_2\text{O}/\text{Na}_2\text{O}$  molar ratio but different  $\text{SiO}_2/\text{Na}_2\text{O}$  molar ratio. The chemical compositions expressed in molar ratios are given in Table 1. For each experiment, the suspension was mixed with a mechanical stirrer 5 min before testing.

### 2.2. Static NMR measurements

Static Nuclear Magnetic Resonance (NMR)  $^{27}\text{Al}$ ,  $^{29}\text{Si}$  and  $^{23}\text{Na}$  experiments were performed on a Bruker Avance500 spectrometer at 11.74 T. The geopolymer paste was placed in an adapted and closed PTFE tube. In practice, the nuclear spin interactions (principally in diamagnetic solid,

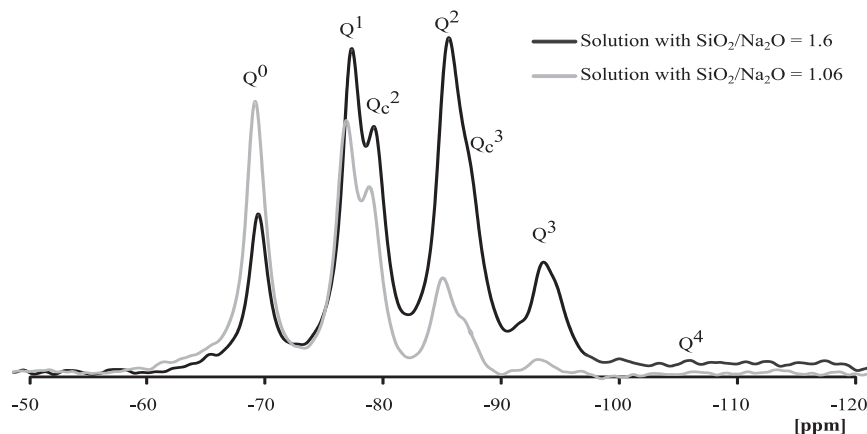


**Fig. 1.** Speciation of silicon in the sodium silicate activation solution by  $^{29}\text{Si}$  NMR.  $\text{Q}^n$  has the usual meaning of the notation commonly used to describe the Si coordination in oxydes [34].

the chemical shift, the dipolar coupling and the quadruple coupling) are anisotropic and the oscillation frequency depends on the orientation of the molecules in the magnetic field. In liquids, Brownian motion naturally averages to zero this anisotropy and high-resolution spectra are obtained. In solid phases however, motional averaging is inexistent and the anisotropy of the interactions leads to a large broadening of the spectra. Therefore, when the bandwidth is adjusted for the observation of species in solution, the solid phases are virtually invisible.

Consequently, in this study, where our sample is a solid/liquid heterogeneous suspension, using static liquid-phase NMR has allowed us to specifically monitor the chemical speciation of the mobile species in the suspending liquid (ions, oligomers or small gel particles).

Three isotopes have been studied,  $^{29}\text{Si}$ ,  $^{27}\text{Al}$  and  $^{23}\text{Na}$ . The  $^{29}\text{Si}$  being a nucleus of spin  $1/2$ , a simple single-pulse sequence  $\pi/2$  was applied. The recycle time of 10 s was greater than five times the longitudinal relaxation time ( $T_1$ ) thus allowing a quantitative analysis of the spectra. The pulse duration was 8  $\mu\text{s}$  and the number of scans 64. The total acquisition time of a spectrum was thus 640 s. The chemical shift external reference was TMS (Tetramethylsilane) at 0 ppm. The diameter of the rf coil is 10 mm.  $^{27}\text{Al}$  is a quadrupolar nucleus (spin  $5/2$ ). However, in the liquid, the quadruple interaction can be neglected and the nutation frequency is comparable to that of a spin  $1/2$ . A simple single-pulse sequence  $\pi/2$  is then non-selective and quantitative. The recycle time was 1 s, the pulse duration  $\pi/2$  4.9  $\mu\text{s}$  and the number of scans 40 (that is acquisition time of 40 s). The external reference, for chemical shift and intensity calibration, was an acidic aqueous solution of 0.10 M  $\text{AlCl}_3$ . The diameter of the rf coil was 5 mm.  $^{23}\text{Na}$  is also a quadrupolar nucleus (spin  $3/2$ ). As for aluminium, the pulses are considered non-selective and quantitative in the liquid phase. For that nucleus, the longitudinal relaxation time was measured through an inversion recovery sequence. The recycle time was 1 s, pulse duration  $\pi/2$  was 5.5  $\mu\text{s}$  and that of the pulses  $\pi$  was 11  $\mu\text{s}$ . The number of scans was 8. The interpulse recovery time was varied between 10 s and 1 s (10  $\mu\text{s}$ , 20  $\mu\text{s}$ , 40  $\mu\text{s}$ , 100  $\mu\text{s}$ , 200  $\mu\text{s}$ , 500  $\mu\text{s}$ , 1.00 ms, 2.00 ms, 4.00 ms, 8.00 ms, 16.00 ms, 32.00 ms, 1 s). The total measurement for a relaxation time  $T_1$  was about 113 s. The external reference for chemical shift and intensity calibration was an acidic aqueous solution of 0.10 M NaCl. The diameter of the rf coil was 5 mm. The samples were weighed and the intensities compared to the integrated intensity of the reference solution; in this manner the intensity of the spectra could be calibrated and expressed in terms of a number of moles of aluminium and sodium.

### 2.3. Rheological measurements

The rheological measurements were carried out with a C-VOR Bohlin® rheometer equipped with a Vane geometry for geopolymer

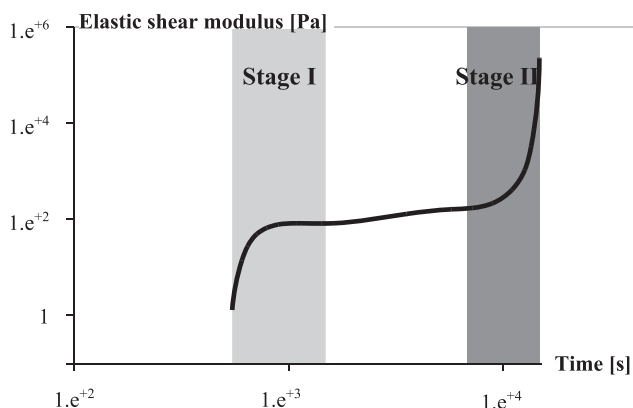


Fig. 2. Elastic shear modulus as a function of time for a geopolymer paste with  $\text{H}_2\text{O}/\text{Na}_2\text{O} = 20$ ,  $\text{SiO}_2/\text{Na}_2\text{O} = 1.06$  and  $\phi = 0.3$ .

mixes. The Vane geometry was chosen to minimise the disturbance of the material during the introduction of the geometry as well as to avoid wall slip [35,36]. For the test on geopolymer mixes, the paste was mixed with a mechanical stirrer for 5 min before immediate transfer into the rheometer's cup. An initial pre-shear at  $100 \text{ s}^{-1}$  was applied during 60 s prior to each test to ensure that all samples were in the same reference state of stress and strain. The elastic shear modulus of the system was then measured by applying strain oscillations of amplitude of  $5 \times 10^{-4}$  and a frequency of 1 Hz. These parameters were shown to allow for non-destructive measurements of the system in the elastic regime in [37]

## 3. Results

### 3.1. Macroscopic observations

While following the evolution of the elastic shear modulus ( $G'$ ) of a MK based geopolymer mix through strain oscillations on the rheometer, a fast increase of the elastic modulus was observed during the first hundreds of seconds and defined as Stage I in Fig. 2. Then, after several hours, another abrupt increase of the modulus was observed defined as Stage II in Fig. 2. A previous study [37] focussed on Stage I and showed that the colloidal interactions between grains are not the main drivers for the early age mechanical properties and first increase of the elastic modulus. This increase was suggested to find its origin in the immediate formation of an aluminosilicate gel "Gel 1" with a rich Al content at the MK grain boundaries.

Mechanically, stage II represented the transition between the liquid and the solid state. The time since mixing associated to this second increase of the modulus could be seen as the beginning of physical setting.

In the following study, we focused on the chemical evolution of the species in the interstitial liquid monitored by static NMR monitoring during stage II.

### 3.2. Monitoring of species by static NMR

#### 3.2.1. $^{27}\text{Al}$ static NMR measurements

Fig. 3 shows the evolution of the aluminium concentration for two compositions. As previously stated in the experimental section, working under static liquid-state NMR, the solid phases provided a  $^{27}\text{Al}$  resonance spectrum too large to be detected and we could consider that most of the detected signal came from the aluminium in the interstitial phase. In practice, the signal was observed in the range of the chemical shift of tetrahedral coordination species (which was expected in view of

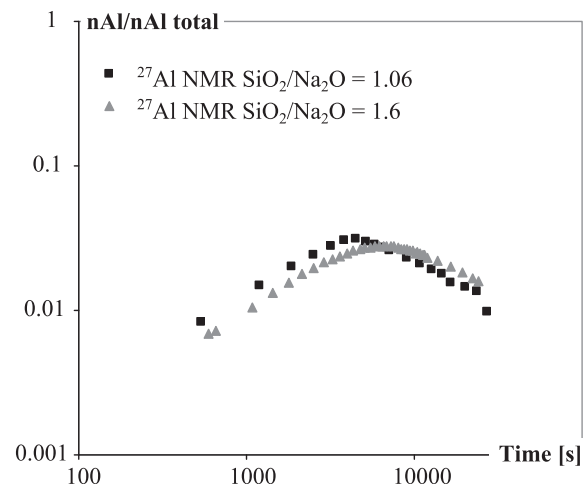


Fig. 3. Evolution of the Al concentration by  $^{27}\text{Al}$  NMR (with  $n\text{Al total} = n\text{Al available in MK}$ ) for two formulations.

the alkaline conditions of the study). It was then integrated and the corresponding value compared to that of a solution reference of known concentration. Knowing the weight of the sample in the rf coil, we obtained the concentration of aluminium. This concentration is ultimately expressed as a proportion of the mass concentration of aluminium in the formulation (namely the one introduced as metakaolin). Two steps were clearly identified. In a first step, the aluminium concentration increases rapidly from zero to about 3% at ~5000 s for the mix with  $\text{SiO}_2/\text{Na}_2\text{O} = 1.06$  and ~7000 s for the mix with  $\text{SiO}_2/\text{Na}_2\text{O} = 1.6$  which was prepared from a water glass solution with a higher chemical modulus. Then, a second step occurred with a slow decay of the aluminium concentration in solution which occurred with an apparent rate similar for both mixes. The decay in Al concentration in the liquid occurred slightly later in the mixes with the lowest alkalinity.

### 3.2.2. $^{23}\text{Na}$ static NMR measurements

Using the same NMR methodology, we followed the evolution of the amount of sodium in the interstitial fluid relatively to the total amount of sodium in the sample. Contrarily to aluminium, sodium is initially exclusively present as a solvated ion and absent from the solid phase. There was a first phase in which the NMR-observable sodium concentration decreased very slowly. After this pseudo-plateau, we observed a sharp drop in the Na concentration in the interstitial fluid. This decrease occurs at a time around 7000 s for the mix with  $\text{SiO}_2/\text{Na}_2\text{O} = 1.06$  and around 10,000 s for the mix with  $\text{SiO}_2/\text{Na}_2\text{O} = 1.6$  (Fig. 4). The observation is remarkably concomitant to the one made by  $^{27}\text{Al}$  NMR with a slight delay for the Na diminution.

During the geopolymerisation, the sodium speciation does not radically change: it is always present as a solvated cation, even in the final geopolymer solid where the sodium is the compensating cation of the negative charge associated with the presence of Al in tetrahedral coordination in the solid network. So, we can suppose that the sodium mobility is strongly conditioned by the integration of Al in a network. Then, when Al is integrated in the geopolymer network, the Na mobility is probably synchronously reduced.

The mobility in the magnetic field being the main cause of relaxation for species in solution, measuring the relaxation time  $T_1$  of sodium allowed us to appreciate the evolution of mobility. In Fig. 5, we observe a steady decrease of the relaxation time right from the start of the preparation of the geopolymer paste. The  $T_1$  of pure silicate solution is close to 5 ms; this allowed us to argue that, sodium was associated to dissolving Al species thus losing mobility. The fact that the evolution of  $T_1$  showed no plateau contrarily to the observed mobile sodium concentration meant that the loss of mobility of sodium is progressive and that an early polymerisation of Al and Si in a first Al rich gel reduces Na mobility even before the solid dense geopolymer phase forms.

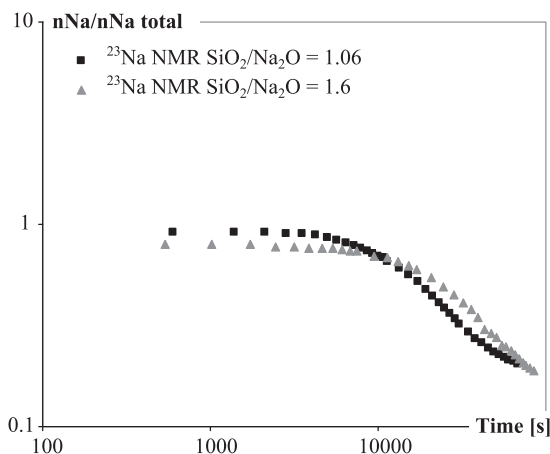


Fig. 4. Evolution of the Na concentration by  $^{23}\text{Na}$  NMR (with  $n\text{Na total} = n\text{Na total}$  in the silicate solution) for two formulations.

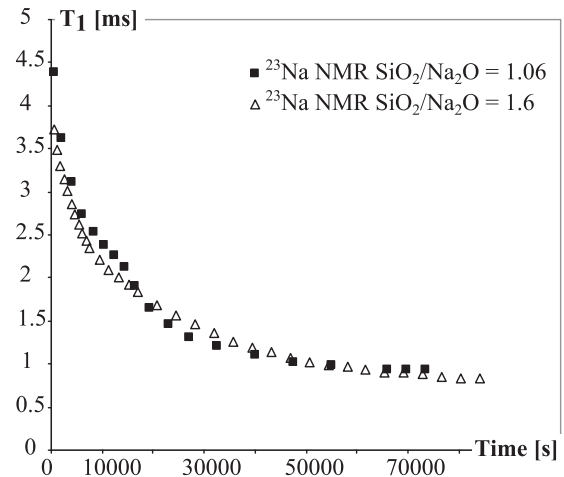


Fig. 5. Evolution of  $T_1$  by  $^{23}\text{Na}$  NMR in the interstitial liquid for different mixes.

### 3.2.3. $^{29}\text{Si}$ static NMR measurements

The same experimental procedure could be followed for the  $^{29}\text{Si}$ . However, while all the aluminium was initially in the MK solid phase, the initial silicon concentration in the activating solution (sodium silicate) is very high and, relatively, the expected concentration changes in the interstitial phase, due to MK dissolution or geopolymer precipitation, are expected to remain marginal in the early stage of development. This aspect, when combined with the poor sensitivity of the  $^{29}\text{Si}$  NMR (low natural abundance of this isotope), prevents us from quantifying the evolution of silicate concentrations in the solution. However, a significant observation is possible: the  $^{29}\text{Si}$  chemical shift changed abruptly with time (Fig. 6). There is a reduction of the resonance around  $-80/-90$  ppm and an increase of the peak to  $-100/-105$  ppm over time (dotted curves in Fig. 6). This shift appeared between 3000 s and 7000 s for the mix with  $\text{SiO}_2/\text{Na}_2\text{O} = 1.06$  and between 13,000 s and 28,000 s for the mix with  $\text{SiO}_2/\text{Na}_2\text{O} = 1.6$ . Therefore, despite the fact that no significant silicon concentration changes can be measured, from the point of view of the silicon speciation, two well separated phases in the geopolymerisation process could nevertheless also be clearly identified.

The speciation of silicon during those two phases can be appreciated by comparison with the large literature on  $^{29}\text{Si}$  NMR studies [34,38,39] on aluminosilicate systems including geopolymer [18,21]. It must be further emphasized that in our experimental conditions (no magic angle spinning MAS), we observe only the species in solution and sub-micron particles animated by a Brownian motion in suspension. The large metakaolin particles were not visible.

This could be understood in terms of the presence of aluminium in the second coordination sphere of silicon, as expected from the rapid

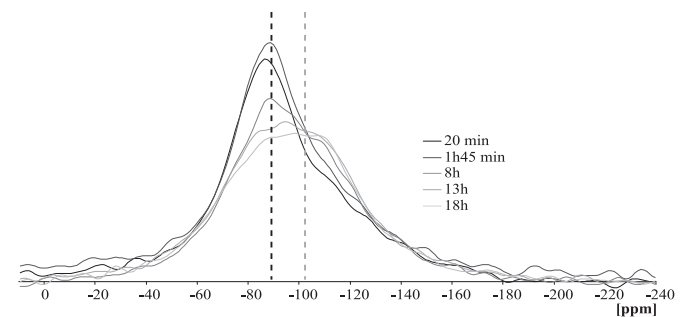


Fig. 6. Evolution of  $^{27}\text{Si}$  NMR spectra for a geopolymer paste with a composition such as  $\text{SiO}_2/\text{Na}_2\text{O} = 1.6$ ;  $\text{H}_2\text{O}/\text{Na}_2\text{O} = 20$  and  $\phi = 0.3$ . The dotted curves represent the chemical shift for the two main peaks over time.



mobilization of aluminium observed by  $^{27}\text{Al}$  NMR. This observation was also in line with the early formation of an Al-rich silica gel observed by Favier et al. [37]. Consequently, we now have, a priori, several types of silicon centres depending on the number of possible aluminium neighbours  $Q^n(m\text{Al})$  (with  $0 \leq n \leq 4$  and  $0 \leq m \leq n$ ). The multiplicity of  $(n,m)$  values in a gel with no local order and the multiplicity of resulting chemical shifts results in a broad unresolved spectrum. Nevertheless, in the first stage, the  $^{29}\text{Si}$  resonance was clearly centred at  $-80$  ppm and signed a low connectivity associated with the occurrence of small size oligomers ( $Q^1-Q^2$ ). Furthermore, a shoulder around  $-105$  ppm showed that species of higher connectivity ( $Q^4(1\text{Al})$  on average) were also already present. This higher connectivity is usually associated with the formation of a gel and thus corresponded to the polymerisation products of the silica–alumina oligomers. Those polymerisation products were small enough to have the sufficient mobility permitting NMR observation without MAS (Magic angle Spinning). Finally, we note that no peak below  $-80$  ppm relative to the presence of Si monomers ( $Q^0$ ) or very small oligomers could be identified in the Si spectra of the interstitial fluid. This is explained by the fact that these species, which were initially present in the solution (see Fig. 1) are the most reactive ones and react rapidly with the Al in solution to form the first Al rich gel reported in the literature [37,40].

So,  $^{29}\text{Si}$  just as  $^{27}\text{Al}$  and  $^{23}\text{Na}$  showed that at least two successive stages could be distinguished during the geopolymerisation reaction. The passage from one stage to the other did not exactly coincide with the perspective of Al or Si speciation in the interstitial phase but this could reflect issues of repeatability and the lower temporal resolution of the  $^{29}\text{Si}$  experiments.

## 4. Discussion

### 4.1. Comparison between the evolution of Al species and Na species

When the temporal evolutions of Na and Al in the interstitial phase are plotted together, it is clear that both elements share the same chemical fate. In Fig. 7, we observe a near perfect match between the evolution of the aluminium concentration and the evolution of the sodium concentration during the second stage occurring after the peak in static-NMR-visible aluminium. This suggested that, in both cases, a similar phenomenon with comparable kinetics occurred. From a practical point of view, sodium is already in the liquid and comes from the activating solution (i.e. not from the dissolved phase). During the geopolymerisation reaction, it is progressively incorporated as a compensating cation in a gel and then in a solid geopolymer network that

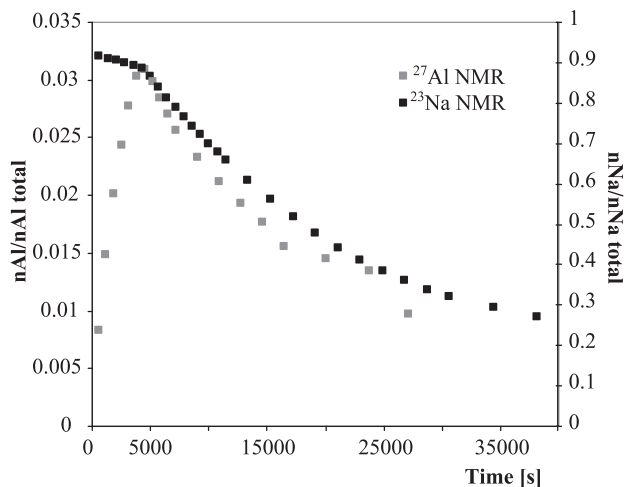


Fig. 7. Comparison between the evolution of Na concentration and Al concentration by  $^{23}\text{Na}$  NMR and  $^{27}\text{Al}$  NMR respectively for a geopolymer paste with a composition such as  $\text{SiO}_2/\text{Na}_2\text{O} = 1.06$ ;  $\text{H}_2\text{O}/\text{Na}_2\text{O} = 20$  and  $\phi = 0.3$ .

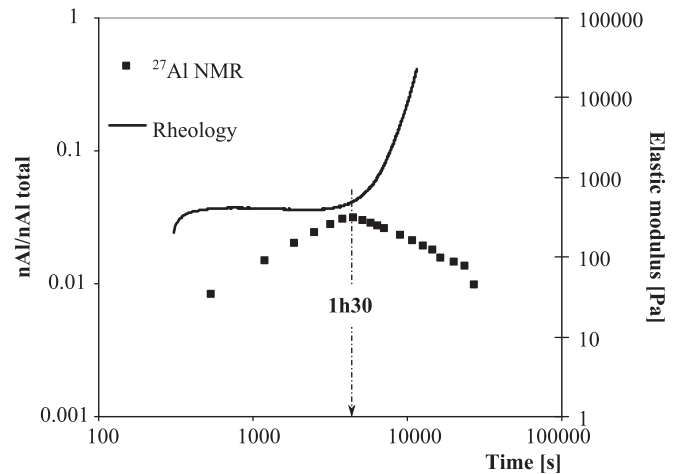


Fig. 8. Comparison between the evolution of Al concentration by  $^{27}\text{Al}$  NMR and the evolution of elastic modulus by rheology of geopolymer with a composition  $\text{SiO}_2/\text{Na}_2\text{O} = 1.06$ ;  $\text{H}_2\text{O}/\text{Na}_2\text{O} = 20$  and  $\phi = 0.3$ .

becomes progressively less visible in NMR as it grows and densifies. Similarly, the Al is incorporated in the new geopolymer in a tetrahedral form and is then associated with a Na compensating ion. However, the Al is not present in the liquid in the beginning of the reaction but is steadily released through the dissolution of the metakaolin. Following sodium concentration allows then to focus only on the incorporation of the Na in a gel with a lower mobility during the second stage. The fact that Al and Na evolved at the same pace is a strong argument in favour of the fact that this second stage of the reaction is linked with the formation of a gel where Al and Na have similar function as in the final geopolymer. Furthermore, no other major changes in the trend of the Na or Al concentration was observed afterward. This showed that the transformation that might occur once the gel is formed after 1 h and 30 min (5000 s) did not occur in the liquid phase.

### 4.2. Comparison with macroscopic observations

Fig. 8 shows the correlation between the two stages identified by NMR and the different periods corresponding to changes in the mechanical properties of the geopolymer paste. After the first increase in elastic modulus and a latent period during which the elastic modulus remained constant, a third period started with a second increase in the elastic modulus which takes place between 5000 s and 7000 s for a geopolymer paste with  $\text{SiO}_2/\text{Na}_2\text{O} = 1.06$ ,  $\text{H}_2\text{O}/\text{Na}_2\text{O} = 20$  and  $\phi = 0.3$ . It can be expected that this increase finds its origin in an increase in the magnitude of the solid particles interactions. As it was shown in [37] that a geopolymeric gel located at the grain boundaries is responsible for the elastic modulus of the geopolymer mixture, an increase in elastic modulus can therefore be attributed to an increase in the elastic modulus of the interstitial gel due to local changes in its chemical composition. Fig. 8 shows that the maximum observed in the concentration of static-NMR-visible aluminium, defining, as described above, the beginning of the second reaction stage, coincides with the second modulus increase. As aluminium and sodium evolution were correlated, this increase in elastic modulus was therefore also correlated with the abrupt decrease of sodium concentration in the liquid. The above results and analysis suggest the precipitation of a denser gel than “Gel 1”, as observed by  $^{29}\text{Si}$  NMR. As a consequence, it seems clear that the formation of this dense gel with high Si connectivity and that incorporates tetrahedral Aluminium linked with a Na compensating cation was linked with an increase of the elastic modulus and was characteristic of the beginning of what can be called the setting of the geopolymer.

### 4.3. Proposition of a phenomenological model for geopolymerisation

The static NMR measurements of Si showed the disappearance in the very early stage after mixing of all  $Q^0$  species in favour of Si species coordinated as  $Q^2$ s. The broadening of the measured peaks indicates Al incorporation in the coordination sphere of the silicon for the silica oligomers in the interstitial phase. We also observe a steady increase in Al concentration in the interstitial phase and a relatively stable concentration of Na (slightly decreasing slope) but an immediate change in the Na mobility indicating the stronger interaction with Al. These observations can be interpreted as the immediate modification of the interstitial liquid activating solution as soon as the metakaolin started to dissolve. The resulting interstitial solution has a higher Si connectivity with Aluminium incorporated in the interstitial phase. As shown previously in [37], this process is strongly heterogeneous and locate at the pseudo contact points between MK grains.

After a period lasting a few thousands of seconds, we observed, in the interstitial phase, a decrease in the Al concentration correlated with a decrease in Na concentration. These evolutions correlate with an increase in the shear elastic modulus of the paste as well as with a higher coordination of Si ( $Q^2 \rightarrow Q^4$ ). All these results suggest a massive precipitation/polycondensation of aluminosilicate specie leading to a solid phase, where Na is incorporated to compensate charges due to Si by Al substitution in a tetrahedral framework. Eventually, all the phases constitutive of the heterogeneous interstitial phase including, but not restricted to the first Al rich gel “Gel 1” and oligomers in solution evolved into a denser “Gel 2” which was static-NMR-invisible.

After this abrupt event, we did not observe other phenomenon involving Al, Na, or Si in the liquid phase. We can therefore suggest that the event occurring around 5000 s was the last major event to explain geopolymerisation. However, it is important to note that reorganisation in “the solid state” remains possible and probably occurred as it has been shown by Fernandez et al. [20] (new gel after 7 days) and explicitly observed by White et al. [30]. Such a reorganisation would not have been observable by the liquid-state NMR methodology followed here.

## 5. Conclusions

Heteronuclear liquid-state NMR allowed a selective observation of the time evolution of Si, Al and Na concentrations and speciations in the interstitial phase, in situ during the geopolymerisation reaction. The results obtained showed a strong correlation between the evolution of Si, Al and Na on the one hand, and the evolution of the mechanical properties on the other hand. This sheds light on some important steps of the geopolymerisation reaction and nicely complemented previous results and models from the literature.

The following phenomenology can be suggested. First, because of MK grains dissolution and Al diffusion in the interstitial phase, an Al rich gel is formed at the grain pseudo-contact points and is at the origin of the first increase in macroscopic elastic modulus [37]. This corresponds to the initial increase in Al in the interstitial phase measurable by static  $^{27}\text{Al}$  NMR and leads to a heterogeneous composition of the interstitial phase.

Then, a massive precipitation/polycondensation of aluminosilicate specie occurs, during which Na is incorporated to compensate the charges of the Al in the tetrahedral framework. Eventually, all the phases constitutive of the heterogeneous interstitial phase including, but not restricted to, the first Al rich gel and oligomers evolves into a denser “Gel 2” which is static-NMR-invisible and the strength increases.

After this abrupt event, we do not observe other any other significant events concerning Al, Na, or Si speciation in the liquid phase. We can therefore suggest that the event occurring around 5000 s is the last major event occurring in the liquid (or gel) interstitial phase and related to geopolymerisation.

Finally, it must be stressed that, given its heterogeneous nature, the system remains highly dependent on all disturbances (i.e. the initial concentrations, duration and energy of mixing, flow history...) [41–43] which could alter the spatial distribution of species. It is therefore particularly difficult to clearly assess the potential number of reorganisations taking place between the first Al rich “Gel 1” and the denser “Gel 2”.

It is therefore particularly difficult to clearly assess the potential number of reorganizations taking place between the first Al rich “Gel 1” and the denser “Gel 2”.

## References

- [1] M. Taylor, C. Tam, D. Gielen, in: IEA International Energy Agency (Ed.) Conference on Energy Efficiency and CO2 Emission Reduction Potentials and Policies in the Cement Industry, Paris, 2006.
- [2] B. Lothenbach, K. Scrivener, R.D. Hooton, *Cem. Concr. Res.* 41 (2011) 1244.
- [3] K.-H. Yang, Y.-B. Jung, M.-S. Cho, S.-H. Tae, J. Clean. Prod. (n.d.).
- [4] K.L. Scrivener, J.-L. Cabiron, R. Letourneux, *Cem. Concr. Res.* 29 (1999) 1215.
- [5] W. Lan, F.P. Glasser, *Adv. Cem. Res.* 8 (1996) 127.
- [6] J. Newman, B.S. Choo, *Advanced Concrete Technology 1: Constituent Materials*, Butterworth-Heinemann, 2003.
- [7] *Magnesia Cement Composition, Process of Its Manufacture, and Composite Comprising Same*, n.d.
- [8] L.J. Vandeperre, M. Liska, A. Al-Tabbaa, *Cem. Concr. Compos.* 30 (2008) 706.
- [9] J. Davidovits, *J. Therm. Anal.* 37 (1991) 1633.
- [10] P. Duxson, J. Provis, G. Lukey, J. Vandeventer, *Cem. Concr. Res.* 37 (2007) 1590.
- [11] P. Duxson, A. Fernández-Jiménez, J.L. Provis, G.C. Lukey, A. Palomo, J.S.J. Deventer, *J. Mater. Sci.* 42 (2006) 2917.
- [12] J. van Deventer, J. Provis, P. Duxson, D. Brice, *Waste Biomass Valoriz.* 1 (2010) 145.
- [13] G. Habert, J.B. d'Espinose de Lacaillerie, N. Roussel, *J. Clean. Prod.* 19 (2011) 1229.
- [14] D. Lambertin, C. Boher, A. Dannoux-Papin, K. Galliez, A. Rooses, F. Frizon, *J. Nucl. Mater.* 443 (2013) 311.
- [15] A. Rooses, P. Steins, A. Dannoux-Papin, D. Lambertin, A. Poulesquen, F. Frizon, *Appl. Clay Sci.* 73 (2013) 86.
- [16] V.F.F. Barbosa, K.J.D. MacKenzie, C. Thaumaturgo, *Int. J. Inorg. Mater.* 2 (2000) 309.
- [17] H. Xu, J.S.J. Van Deventer, *Int. J. Miner. Process.* 59 (2000) 247.
- [18] A. Bourlon, *Physico-Chimie et Rhéologie de Géopolymères Frais Pour La Cimentation Des Puits Pétroliers*, Université Pierre et Marie Curie, 2010.
- [19] J.L. Provis, G.C. Lukey, J.S.J. van Deventer, *Chem. Mater.* 17 (2005) 3075.
- [20] A. Fernandez-Jimenez, R. Vallepu, T. Terai, A. Palomo, K. Ikeda, *J. Non-Cryst. Solids* 352 (2006) 2061.
- [21] P. Duxson, J.L. Provis, G.C. Lukey, F. Separovic, J.S.J. van Deventer, *Langmuir* 21 (2005) 3028.
- [22] M. Xia, H. Shi, X. Guo, *Mater. Lett.* 136 (2014) 222.
- [23] M.R. Rowles, J.V. Hanna, K.J. Pike, M.E. Smith, B.H. O'Connor, *Appl. Magn. Reson.* 32 (2007) 663.
- [24] J. Tailby, K.J.D. MacKenzie, *Cem. Concr. Res.* 40 (2010) 787.
- [25] Y.-L. Tsai, J.V. Hanna, Y.-L. Lee, M.E. Smith, J.C.C. Chan, *J. Solid State Chem.* 183 (2010) 3017.
- [26] F. Zibouche, H. Kerdjoudj, J.-B. d'Espinose de Lacaillerie, H. Van Damme, *Appl. Clay Sci.* 43 (2009) 453.
- [27] M. Rowles, B. O'Connor, *J. Mater. Chem.* 13 (2003) 1161.
- [28] C.E. White, J.L. Provis, A. Llobet, T. Proffen, J.S.J. van Deventer, *J. Am. Ceram. Soc.* 94 (2011) 3532.
- [29] C.E. White, K. Page, N.J. Henson, J.L. Provis, *Appl. Clay Sci.* 73 (2013) 17.
- [30] A. Buchwald, H.-D. Zellmann, C. Kaps, *J. Non-Cryst. Solids* 357 (2011) 1376.
- [31] H. Rahier, J. Wastiels, M. Biesemans, R. Willems, G. Assche, B. Mele, *J. Mater. Sci.* 42 (2006) 2982.
- [32] P. Duxson, J.L. Provis, G.C. Lukey, S.W. Mallicoat, W.M. Kriven, J.S.J. van Deventer, *Colloids Surf. A Physicochem. Eng. Asp.* 269 (2005) 47.
- [33] G. Engelhardt, D. Hoebbel, M. Tarmak, A. Samoson, E. Lippmaa, *Z. Anorg. Allg. Chem.* 484 (1982) 22.
- [34] P. Coussot, *Rheometry of Pastes, Suspensions, and Granular Materials*, Wiley-Interscience, Hoboken (N.J.), 2005.
- [35] A.W. Saak, H.M. Jennings, S.P. Shah, *Cem. Concr. Res.* 31 (2001) 205.
- [36] A. Favier, G. Habert, J.B. d'Espinose de Lacaillerie, N. Roussel, *Cem. Concr. Res.* 48 (2013) 9.
- [37] G. Engelhardt, U. Lohse, A. Samoson, M. Mägi, M. Tarmak, E. Lippmaa, *Zeolites* 2 (1982) 59.
- [38] R.K. Harris, C.T.G. Knight, *J. Chem. Soc. Faraday Trans.* 2 79 (1983) 1525.
- [39] K. Sagoe-Crentsil, L. Weng, *J. Mater. Sci.* 42 (2006) 3007.
- [40] A. Favier, *Mécanisme de Prise et Rhéologie de Liants Géopolymères Modèles*, Université Paris-Est, 2013.
- [41] M. Palacios, F. Puertas, *ACI Mater. J.* (2011) 73.
- [42] A. Favier, J. Hot, G. Habert, N. Roussel, J.-B. d'Espinose de Lacaillerie, *Flow properties of MK-based geopolymer pastes. A comparative study with standard Portland cement pastes*, *Soft Matter* (2014) <http://dx.doi.org/10.1039/C3SM51889B>.
- [43] M. Palacios, P.F.G. Banfill, F. Puertas, *Rheology and setting of alkali-activated slag pastes and mortars: effect of organic admixture*, *ACI Mater. J.* 105 (2008) 140–148 (<http://cat.inist.fr/?aModele=afficheN&csid=20274581> (accessed June 9, 2011)).